



The Use of Electrical Resistivity Tomography to Investigate Basaltic Lava Tunnel Based on the Case Study of Al-Badia Cave in Jordan

¹HANI AL-AMOUSH and ²JAFAR ABU RAJAB

¹Institute of Earth and Environmental Sciences, Al al-Bayt University, Mafrqa, Jordan

²Faculty of Natural Resources and Environment, Department of Earth Sciences and Environment, Hashemite University, Zarqa, Jordan

Corresponding author: hani.alamoush1@gmail.com

Manuscript received: January 11, 2018; revised: April 4, 2018;

approved: June 5, 2018; available online: August 6, 2018

Abstract - Electrical Resistivity Tomography (ERT) was employed to conduct a geoelectrical survey near the Al-Badia lava tunnel located close to the Al-Bishyria Village in Jordan. The technique enabled the mapping of the subsurface tunnel extension and description of its inner structure. To assess the quality of data and resistivity models, Schlumberger and Reciprocal Schlumberger electrode configurations were used to produce eight ERT profiles. As revealed by the examination of received potential, the implemented configurations exhibited a strong signal, producing an approximated reciprocal error of up to 6%. The findings of ERT models showed that the lava tunnel had a clearly outlined structure with an elliptical to rectangular shape. The modelled resistivity of the lava tunnel was obtained in proximity to 1000 Ω -m, with a better characterization being possible at resistivity exceeding 8000 Ω -m in 200 Ω -m of Fahda Vesicular Basalt medium. An exploration depth of 50 m revealed that the lava tunnel was 10 m deep and 5 m in diameter on the average. Furthermore, potential means of groundwater recharging were reported by the simultaneous detection of a number of resistivity anomalies of less than 50 Ω -m and lava tunnel. In addition, the lava tunnel was observed to extend and ramify beyond the area under investigation, indicating at the potential existence of multiple lava tunnel extensions in both the investigation area and in the basaltic flows, which could have adverse implications for future urban projects.

Keywords: lava tunnel, ERT, basaltic flow, Jordan

© IJOG - 2018. All right reserved

How to cite this article:

Al-Amoush, H. and Rajab, J.A., 2018. The Use of Electrical Resistivity Tomography to Investigate Basaltic Lava Tunnel Based on the Case Study of Al-Badia Cave in Jordan. *Indonesian Journal on Geoscience*, 5 (2), p.161-177. DOI: [10.17014/ijog.5.2.161-177](https://doi.org/10.17014/ijog.5.2.161-177)

INTRODUCTION

Located in north-eastern Jordan, the intra-plate Harrat Al-Shaam Basalt of Neogene-Quaternary period is believed to be the northern extension of the north Arabian province (Ibrahim *et al.*, 2001). Spanning a distance of over 3,000 km, it spreads north-south in alignment to the Red Sea axis, from Syria through Jordan to Saudi Arabia (Figure 1a) (Kempe *et al.*, 2012). Jordan com-

prises 11,000 km² of around 46,000 km² of overall surface area (Ibrahim, 1997), earning it the status of the volcanic field of the greatest size in the Arabian Plate (Ibrahim and Al-Malabeh, 2006). The basaltic volcanic province of North Arabia has been the focus of extensive researches (*e.g.* Lartet, 1869; Doss, 1886; Van Den Boom and Sawwan, 1966; Bender, 1968, 1974; Abed *et al.*, 1985; Al-Malabeh, 1989, 1994; Ibrahim, 1993a, 1996a, 1996b, 2000; Ibrahim and Hall, 1995,

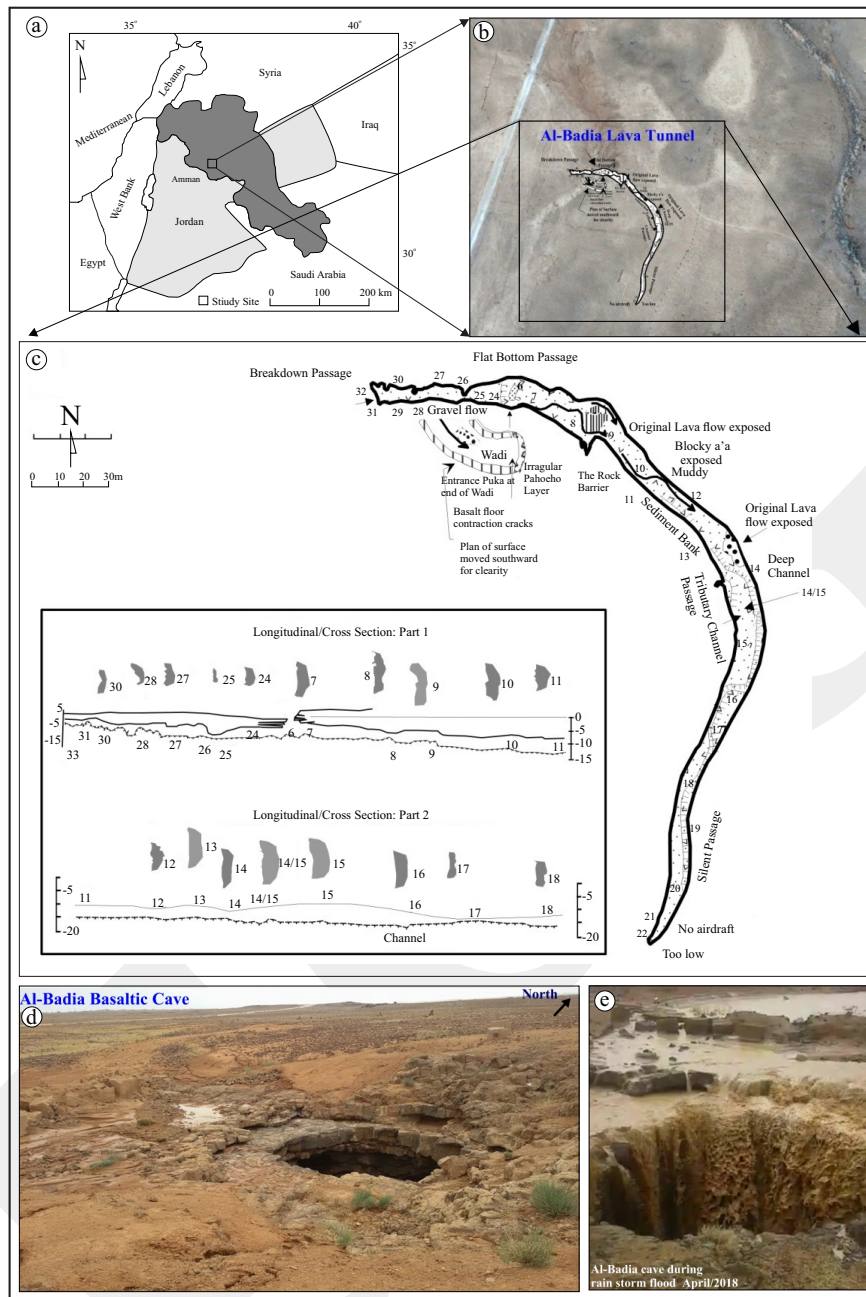


Figure 1. Jordan map showing the: a. Harrat Al-Shamm Basalt; b. Schematic representation of the inner structure of the Al-Badia lava tunnel (modified after Kempe *et al.*, 2006) superimposed on a Google Earth map; c. Schematic representation of the inner configuration of the Al-Badia lava tunnel (modified after Kempe *et al.*, 2006); d. General view of Al-Badia Basaltic Cave; e. Rainstorm flood at Al-Badia basaltic cave (photo taken from Al-Adamat, 2018).

1996). The Natural Resource Authority (NRA) has comprehensively mapped the geology of this province (Ibrahim *et al.*, 2001). The Harrat Al-Shaam basaltic super group is a classic intra-plate continental basaltic flow of alkali olivine basalt comprising the basaltic provinces and are classified into five groups (Ibrahim, 1993a). The K-Ar dating method produced a date of between 13.7

Ma to less than 0.5 Ma for the volcanic activity in northeastern Jordan (Barberi *et al.*, 1979; Moffat, 1988; Tarawneh *et al.*, 2000; Illani *et al.*, 2001).

In northeastern Jordan, basaltic lava flows are arranged in sedimentary successions in an unconformable way. Within the studied area, the direction of these flows is approximately to the south and southeast, as shown in Figure 2a. Basaltic

lava is not homogeneously thick; for example in Syria, it has a thickness of about 1 km, but at the border between Jordan and Syria it is around 600 m thick, and its thickness decreases to the south, becoming interspersed with sediments (Gibbs, 1993). Geological field surveys conducted by Bender (1968) and Al-Dmour (1992) uncovered a number of basaltic lava flows, with a minimum of fourteen basaltic lava flows of different thickness being discovered in the north of the Azraq Basin by deep penetration drilling (NRA, 2008). In the area of the Harrat Al-Shaam, surveys and explorations of several basaltic lava caves carried out, have been adequately mapped and documented (Arsalan, 1974; Al-Malabeh, 2005; Kempe *et al.*, 2012). Kempe *et al.* (2012) extensively investigated twenty such caves, then describing their locations and extensions and categorizing them into types in accordance with how they were formed and their inner structures, including lava tunnel (pyroduct), pressure ridges, which some of them are of unknown origins.

Lava tubes, lava tunnels, and volcanic structures in different parts of the world have been the focus of multiple geophysical studies. For instance, the lava tube in the northeastern Jordanian region of Umm Al-Quttain has been

explored by Al-Oufi (2006) and Al-Oufi *et al.* (2012) with the two-dimensional techniques of induced polarization imaging (2D-IP). The extension of two lava tube faults and dikes in northeastern Jordan was investigated by Al-Oufi *et al.* (2008) based on a very low frequency (VLF) electromagnetic technique. Moreover, the techniques of ground penetration radar (GPR) and electrical resistivity imaging (ERI) were combined by Ortiz *et al.* (2007) to explore volcanic materials and features in Tenerife, Spain. GPR was also used by Miyamoto *et al.* (2003) to identify lava tubes in the Komoriana Cave at the Fuji Volcano, Japan. Detection of volcanic structures of superficial depth in a region of high potential value was conducted by Ortiz *et al.* (2014) within various geophysical prospecting techniques, such as microgravity, GPR, and electromagnetic induction (EMI). The lava tunnel of Manjanggal on Cheju Island was investigated by Kwon *et al.* (1998) through different geophysical techniques.

The purpose of the present study was to explore the shallow structures of the Al-Badia lava tunnel in the Al-Bishriyya region, Jordan based on electrical resistivity tomography (ERT). A comprehensive assessment of the efficiency of

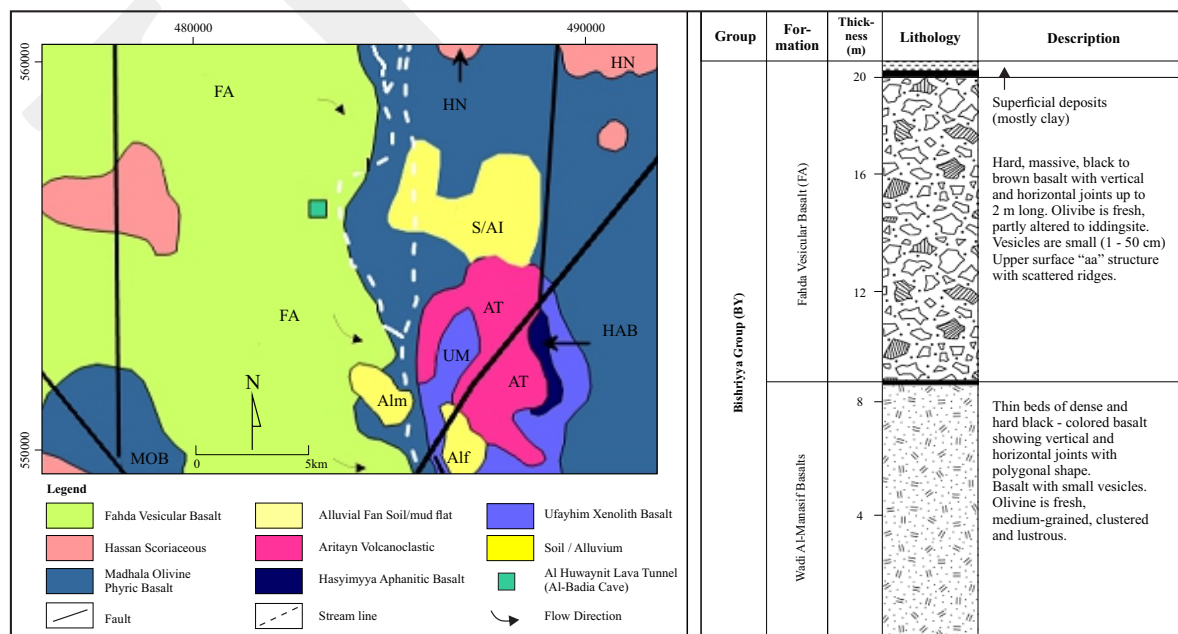


Figure 2. a. Simplified geological map of the studied area (Modified after Ibrahim, 1997); b. Columnar log description for BY (Bishriyya Group) (Ibrahim *et al.*, 2001).

two-dimensional resistivity data obtained in the researched area was undertaken with regard to data quality and resistivity models. Furthermore, to determine whether the underground lava tunnel structure could serve as a source of groundwater recharge in an area of high aridity, the extensions of the lava tunnel were investigated through the resistivity models.

Research Area

To ascertain the usefulness of ERT for exploration of known tunnel subsurface extensions, the present study focused on the case study of the Al-Badia Cave. Otherwise, referred to as the Al-Huwinit or Beer Al-Hamam cave, this cave received its name from Al-Malabeh (2005), and it is considered to be a lava tunnel basaltic cave (Kempe *et al.*, 2012). Based on the WGS 1984 coordinate system, the coordinates of the cave are 32°07'57.06"N and 36°49'25.14"E, which is in the proximity of the Al-Bishriyya Village (Figure 1). Kempe *et al.* (2006) conducted a comprehensive survey of the cave with the purpose of mapping its inner structural features. The subsurface extension and the inner features of the Al-Badia lava tunnel are represented in a schematic form in Figures 1b and 1c (Kempe *et al.*, 2006).

The Al-Badia lava tunnel has an overall volume of 20,000 m³ (Shawaqfah *et al.*, 2014), 15 m wide and of 8 m high. Its access point is a roof collapse (Figure 1d) with a depth of 5 m. Its location on the path of an important wadi means that, during rainfall, it is gradually filled with fine sediments and loess transported by the running water (Figure 1e), that are thick enough to block its extension (Al-Malabeh *et al.*, 2012). A survey and mapping were conducted on just 445 m of the tunnel (Kempe *et al.*, 2012), but its subsurface extensions are anticipated to be larger. Groundwater recharge depends greatly on the high volumes of surface water stored by the lava tunnel during floods (Figure 1e) (Al-Amoush, 2010; Shawaqfah *et al.*, 2014). A simulation of the groundwater was undertaken by Shawaqfah *et al.* (2014), revealing that the storage of surface water by the Al-Badia lava tunnel led to an increase of 0.2 - 0.5 m in the level of local groundwater.

As suggested by Al-Malabeh (2005), the lava tunnel may have potential uses in the context of environmental tourism.

Geological Characteristics of the Research Area

The geology of the studied area is mapped in a basic form as shown in Figure 2a (Ibrahim, 1997). The area is composed of several geological formations (Ibrahim, 1997).

Dating to the Pleistocene-Holocene, the Bishriyya Group (BY) consisting of the latest volcanic activity in northeastern Jordan, is associated with the majority of B6 basalt classified by Van Den Boom and Sawwan (1966) and Bender (1974). According to the truncation of flow lines that showed distinct ages, the group is separated into two formations, namely, the upper division of Fahda Vesicular Basalt Formation (FA) and the lower division of Wadi Mansif Basalt Formation (WMF). The WMF is not exposed in the studied area as indicated on the map (Figure 2a). On the north side, BY projects from volcanic vents is flooded along earlier wadis. A columnar log description of BY in the researched area is provided in Figure 2b (Ibrahim *et al.*, 2001). From a morphological perspective, BY consists of fresh blocky "aa" and some "pahoehoe" flows. The direction of the basalt lava flow is indicated by a number of pressure ridges, which present shrinkage joints with a width of up to 50 cm and length of 6 m that are usually considered to be the products of cooling of basaltic lava. Furthermore, polygonal columnar jointing is another characteristic feature, and records of preserved lava tubes have been made at numerous sites within this group in Umm El-Quttain region. The phenocrysts making up BY are melanocratic grey, with fine grains, and colour that varies between green and yellowish olivine (Ibrahim *et al.*, 2001). The K-Ar isotope dating technique produced a date of between 1.45 Ma to less than 0.1 Ma for the FA formation (Baraberi *et al.*, 1979 and Moffat, 1988). However, Tarawneh *et al.* (2000) obtained an age range that differed somewhat, between 3.5 Ma to less than 0.5 Ma.

METHODOLOGY

Strategy of Field Survey and Data Collection

Two-dimensional resistivity data were obtained at eight sites in the area of Al-Badia tunnel cave with the multi-electrode 2D-ERT technique (Figure 3). The strategy of field data collection was geared towards attaining a representative resistivity signature of subsurface tunnel structures by executing a number of profiles throughout or near the lava tunnel. Apart from the 2D-ERT profiles of ERT04 and ERT06, which were oriented in east-west direction, the other five profiles of ERT01, ERT02, ERT03, ERT05, and ERT07 were oriented mainly in a north-south to northeast - southwest directions (Figure 3a). Furthermore, the profiles carried out from potential lava tunnel extensions that were not known were ERT06 and ERT07 (Figure 3a). Resistivity was measured by Syscal Junior Switch instrument (Figure 3c) via forty-eight electrodes which were arranged at 5 m electrode spacing.

Every 2D-ERT profile was 235 m long, and for all conducted profiles, Schlumberger (S) and Reciprocal Schlumberger (RS) configurations were employed. RS indicates where the injection current electrodes are relatively located internally towards the middle of the array, while the position of receiving potential electrodes is external to electrical current electrodes. By contrast to the standard Schlumberger array, this configuration exchanged current and potential pairs, so that the configuration factor K stayed unchanged (Figure 3b).

At the studied area (Figure 1d, 3c), lava tunnel outcrop appears as an air-filled cavity structure overlain by superficial clay deposit layers. This model makes the ground condition to be highly conductive over highly resistive cavity structure. The Schlumberger (S) configuration was applied, because it was characterized by good depth of penetration and resolution where the applied current and received signals are of high signal-to-noise ratio (S/N) (Loke, 2013). Moreover, the S

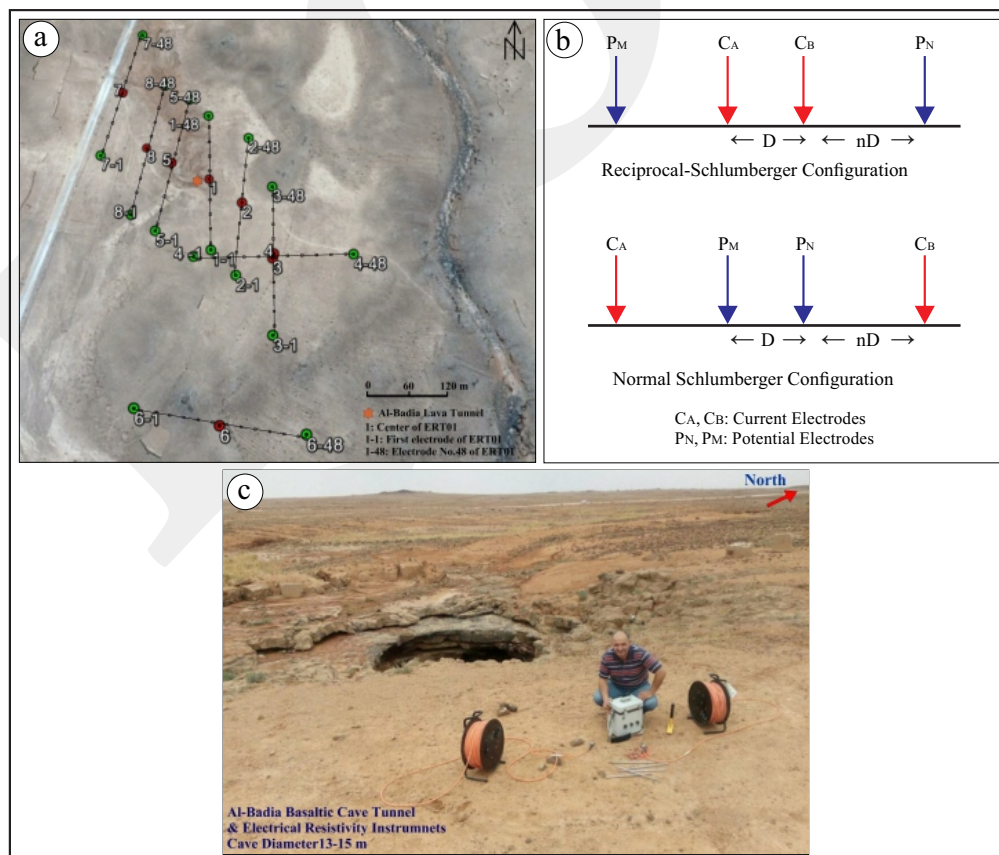


Figure 3. a. Map showing the position of ERT profiles in the researched area and their orientation; b. The configurations of the employed electrical electrodes; c. Al-Badia basaltic cave and ERT instruments.

configuration has a slightly better spatial resolution than other common resistivity configurations (*i.e.*, Dipole-Dipole and Wenner configurations) which make it becomes sensitive to resolve high-resistivity structure at comparable models. In addition, RS configuration tends to quantify random noise at larger values as it picks up more noises, being useful to assess such noises at higher levels (Dahlin and Zhou, 2004). The choice of S and RS model-based configurations implemented at this study can be compared and assessed by the synthetic model composed of high-resistive buried channel embedded in conductive structures (similar to our lava tunnel model) presented by Dahlin and Zhou (2004). Their resistivity model-based S configuration shows a good resolution of buried channel at low noise contamination where S/N is quite high. The derived model also has accurately resolved and mapped the overburden layer of moderate conductivity.

The ERT is designed in such a way that makes it possible to record 565 quadripoles arranged over 21 levels, and has an apparent penetration depth of around 50 m. Between the first and 21st resistivity level, K varies from 31.42 m to around 2061.67 m.

Quality of Data and Evaluation of Errors

The noise of the resistivity measurements can be approximated by determining a quality factor based on an observed potential error (*i.e.* reciprocity error), derived from the normal measurements attained from S configuration and the reciprocal measurements attained from RS configuration. To obtain the 1% standard deviation of the calculated potential, the configuration of the instrument system is set on acquisition of resistivity measurements (*i.e.* quadripoles) at six stacking, current pulse length of 1.0 s, and instrument voltage of 800 V.

Ground resistance of less than 9 k Ω was exhibited by the obtained resistivity data, with around 200 mA maximum injected current and received potential attained at the highest value of 55 mV driven by instrument power up to 400 V.

Apart from the quadripoles, which displayed significant disturbances close to the first level equivalent to an apparent depth of 2.85 m, a less

than 6% stacking error arose in the conducted survey. The fact that the superficial conductive clay layer and the resistive layer underneath (Fahda Vesicular Basalt formation) came into contact might explain the disturbances.

The stacking error is typically lower compared to the reciprocal error (Binely *et al.*, 1995). Noise content and magnitude in resistivity pseudo-section can be better estimated based on reciprocal error, whereas the data quality afforded by the low stacking error is poor (Zhou and Dahlin, 2003). A direct correlation may be established between a number of intrinsic errors and various sources; to give an example, background noises of an ambient and anthropogenic nature, physical instrument dysfunction, and high contact resistance of electrodes used in measurements, which supply a source of excess and non-linear potential dominate imaging results (Ramirez *et al.*, 1999; Zhou and Dahlin, 2003; Wilkinson *et al.*, 2008).

As shown in Figure 4, the reciprocal errors of the eight ERT profiles take the form of a logarithmic plot of absolute relative potential errors, the calculation of which is based on the normal and reciprocal measured potential. The plot comprises statistical parameters such as mean M and fitting regression line as well; for instance, reciprocal error for the illustrated data was defined and quantified based on standard deviation SD .

By examining the relative potential errors, it was found that outliers have a suboptimal performance in the part of the plot (Figure 4) associated with measured potential of less than 1 mV, while other outliers were related to a relative potential error exceeding 15%. On the whole, by analyzing the potential errors of the eight ERT profiles, it could be observed that the employed configurations had suitable signal strength, since the majority of measured data were in the region of 10-15 mV of measured potential error.

The reduction in the relative potential error due to the rise in the measured potential up to 15 mV resulted in a negative trend in the regression lines. The SD of the relative potential errors (%) in the range 2.9 - 6% was used for representation of the attained reciprocal error.

The Use of Electrical Resistivity Tomography to Investigate Basaltic Lava Tunnel Based on the Case Study of Al-Badia Cave in Jordan (H. Al-Amoush and J.A. Rajab)

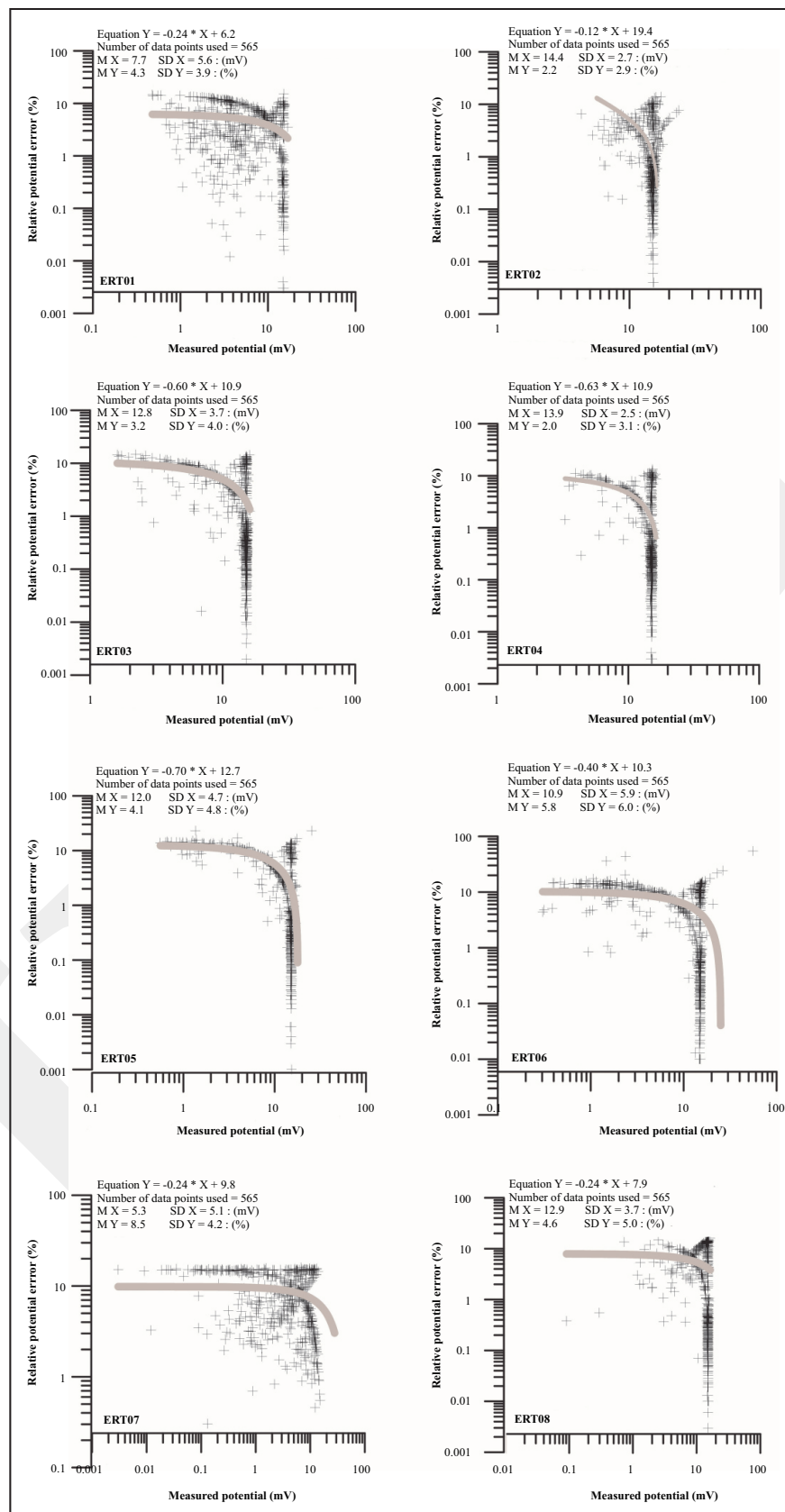


Figure 4. Potential errors derived from normal and reciprocal measurements associated with the eight ERT profiles represented in a logarithmic plot. The *SD* of relative potential error produced a reciprocal error in the range of 2.9 - 6% between ERT02 and ERT06. The plot shows the regression line and statistical parameters as well.

For each ERT profile, relative resistivity pseudo-sections were created in order to enable understanding of how the relatively measured potentials and their sequential apparent resistivity values were spatially assessed (Figure 5). The results show that the majority of plotted data were observed to be within $\pm 4\%$ of resistivity variations and were congruent with around 90% of reciprocal data. Several high-positive or high-negative noisy data occurred in localized zones throughout and at the side of pseudo-sections (*i.e.* ERT03 and ERT05). In addition, a correlation existed between numerous noisy data and greater depths, with measurement of noises at the longer potential electrode separation or large K values (*i.e.* ERT02, ERT06, and ERT08). Random noisy data dominated at every level of measured data, as exhibited by some relative resistivity pseudo-sections (*i.e.* ERT01, ERT06, and ERT07).

Inversion of Resistivity Data

As noted by Kempe *et al.* (2006), the manner in which basaltic lava was geologically constituted and how it was structured underground revealed that a lava tunnel was an inhomogeneous three-dimensional feature with regard to depth, form, and the occurrence of bulk spaces that loaded with fine sediments. Non-random sources produce the noises in the outliers present in the resistivity datasets. Given that the reciprocal errors demonstrated by all the resistivity data were less than 10%, the impact of outliers on the resistivity measurements was minimized through the application of the blocky or robust inversion routine. The purpose of the robust resistivity model accompanying the L_1 -norm inversion is to reduce the absolute difference between the measured and calculated apparent resistivity values as much as possible (Loke *et al.*, 2003). RES2DINV software permitted inversion of the resistivity data (Loke, 2002), and the quality indicator of inverted models was taken to be the root mean squared error value (RMSE %). The most common usage of robust inversion is in detection and refinement of sharp boundary over pronounced resistivity contrast (Loke, 2002). Furthermore, smoothness-constrained least square

inversion, which is characterized by the fact that the L_2 -norm inversion displays sensitivity to outliers (de Groot-Hedlin and Constable, 1990) was employed as well in this study. A relatively higher RMSE value was obtained from this inversion, generating comparable resistivity image of major signatures, despite the slight change in the resistivity scale and less resolved areas of sharp resistivity contrast (Figure 6a).

To give an example, the implication of the ERT01 pseudo-resistivity section conducted in the proximity of exposed lava tunnel is that resistivity distributed with a clear interface among various regions at distinct resistivity values and the resistivity value in every region is smooth and constant (Figure 6b). An anomaly with an ellipsoidal form and high resistivity ($\sim 1,000 \Omega\text{-m}$) was found to develop between the horizontal distance of 90 m and 110 m at approximately 5 m depth, according to the robust resistivity model. Furthermore, numerous sites were found to have conductive features ($\sim 50 \Omega\text{-m}$) close to the surface, which could have been linked to similar deep conductive features under the anomaly of high resistivity. The robust resistivity model provides a satisfactory explanation for this. It is worth noting that due to the three-dimensional effect that lava tunnel implies, such setting can give rise to artifacts in the resolved model as a two-dimensional forward scheme used for modeling of the three-dimensional structure (Griffiths and Barker, 1993).

Interpretation of Data and Results

The inverted resistivity data took seven iterations to achieve convergence of the resistivity models of the ERT profiles, and the associated RMSE values of less than 7.7% were constrained and retained their prominence with the reciprocal data error, considering that the proportion of data filtering was around 8% (Figure 7). Since logarithmic variations in resistivity values are known to occur, a fixed logarithmic colour scale was employed to present each resistivity model, thus enhancing clarity and enabling comparative analysis between the models. There was consistency between the ERT01 model and the inner

The Use of Electrical Resistivity Tomography to Investigate Basaltic Lava Tunnel Based on the Case Study of Al-Badia Cave in Jordan (H. Al-Amoush and J.A. Rajab)

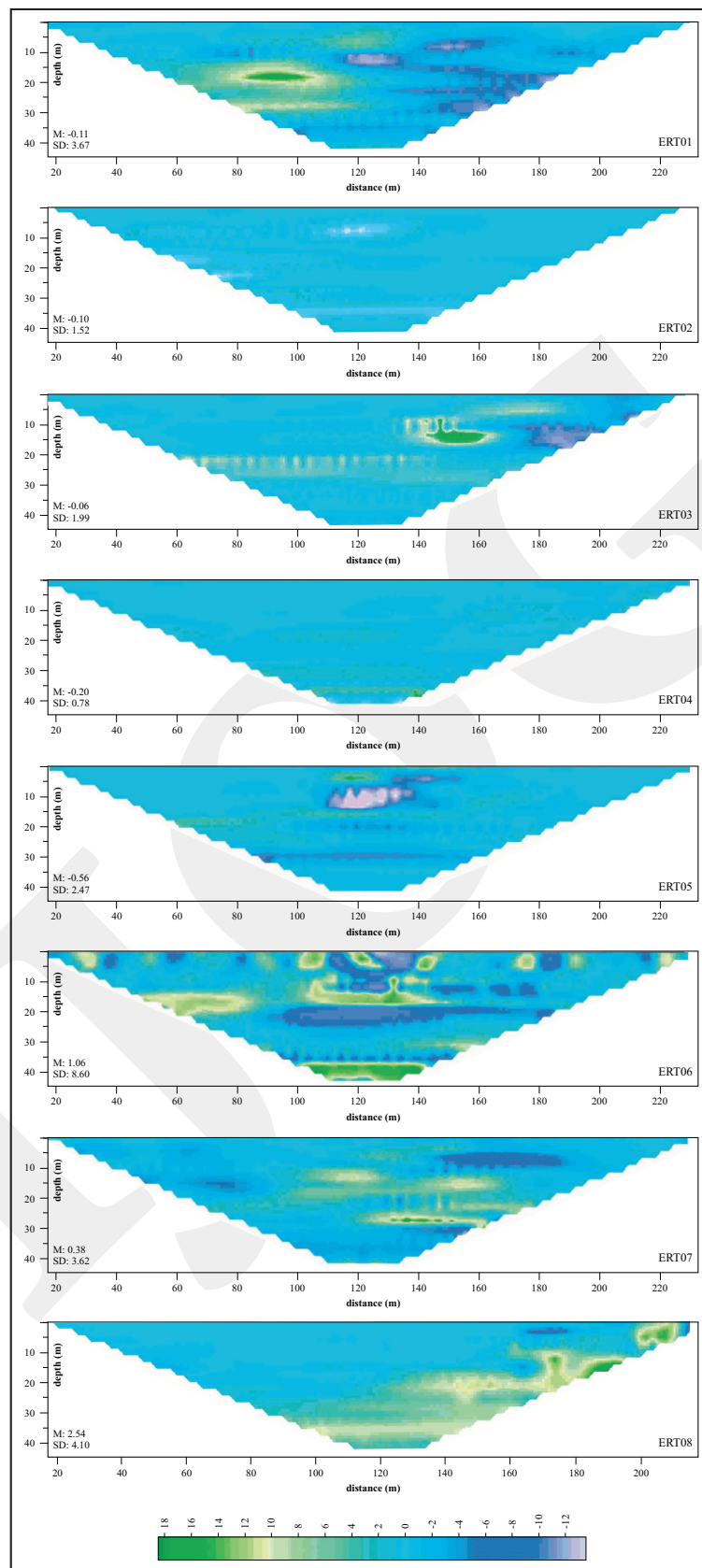


Figure 5. Relative resistivity variation ($\Omega\text{-m}$) derived from the measurements of normal and reciprocal resistivity for the eight ERT profiles shown in pseudo-sections; these measurements have an *SD* in the range of 0.78 (ERT04) and 8.6 (ERT06), while the general *M* is around 1%.

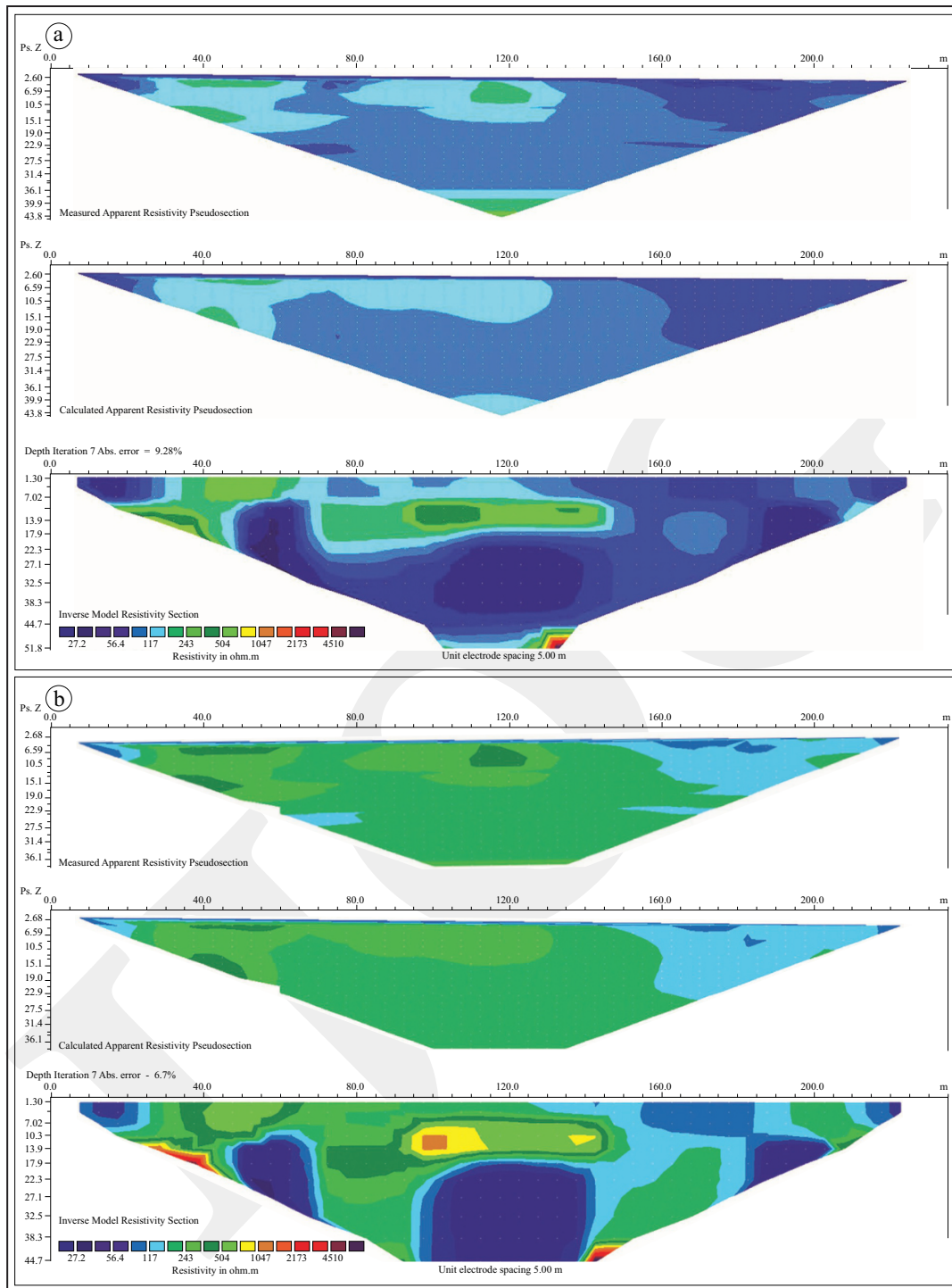


Figure 6. a. Resistivity model associated with smoothness-constrained least square inversion at ERT01, with 9.28% RMSE for L_2 -norm inversion according to the plot of calculated and measured resistivity data. The acquisition of the inverted models occurred after 7.8% cut-off noisy data; b. Resistivity model associated with the robust inversion at ERT01, with 6.7% RMSE for L_1 -norm inversion, according to the plot of calculated and measured resistivity data.

structure at the collapsed ceiling section of the lava tunnel. The air-filled lava tunnel with a diameter of 5 m representing anomaly “A” was defined by $\sim 1000 \Omega\text{-m}$ and positioned 5 m deep in

the medium of $\sim 200 \Omega\text{-m}$ of the Fahda Vesicular Basalt Formation. The floor of the lava tunnel is flat in this area, with basaltic contraction cracks (Figure 1c) (Kempe *et al.*, 2006) and the forma-

The Use of Electrical Resistivity Tomography to Investigate Basaltic Lava Tunnel Based on the Case Study of Al-Badia Cave in Jordan (H. Al-Amoush and J.A. Rajab)

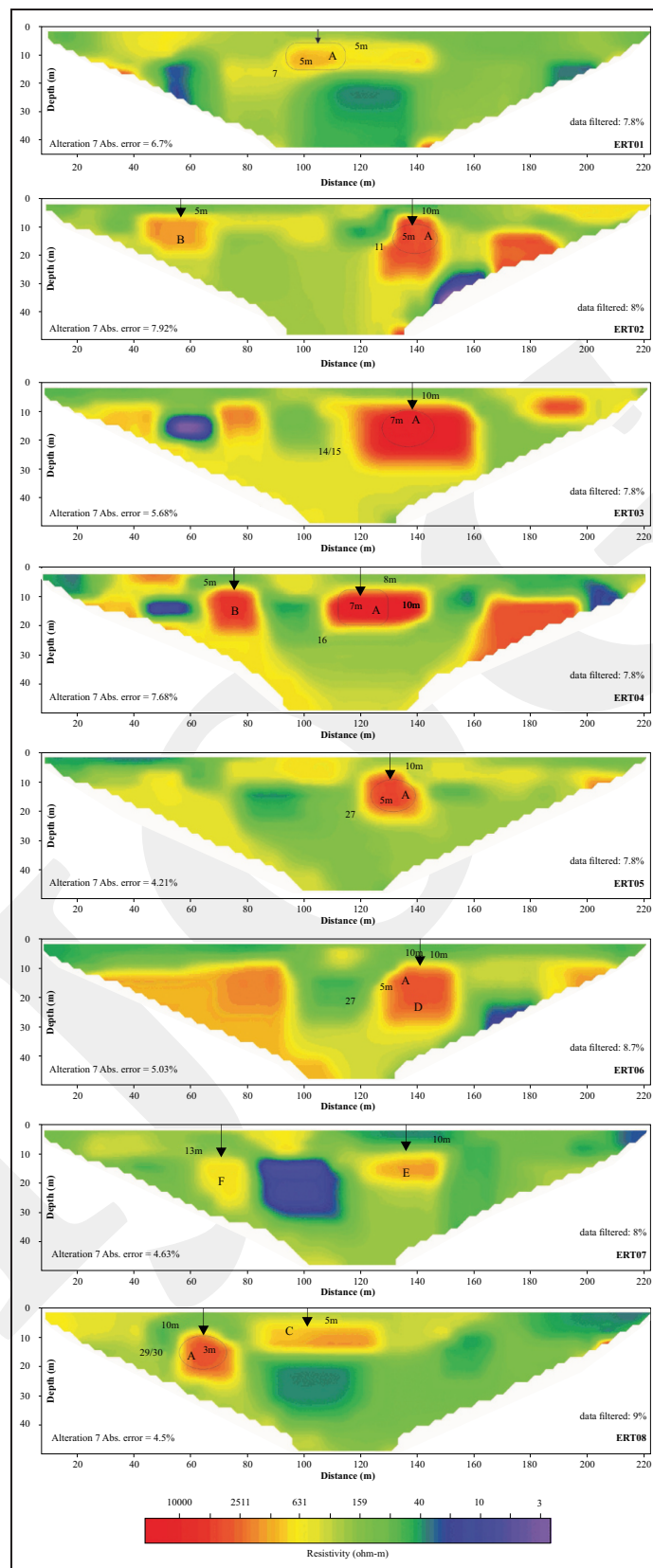


Figure 7. Resistivity models associated with the resistivity profiles; according to the underground map, the known lava tunnel is indicated by anomaly “A” (Kempe *et al.*, 2006), while anomalies “B”, “C”, “D”, and “F” may represent extensions of “A” or new lava tunnels. The numbers next to the anomalies (*i.e.* 7, 11, 14/15, 16, 27, 29/30) indicate how the anomalies of the ERT profiles and their positions are spatially coordinated and correlated in plan view and longitudinal cross-section (Figure 1c).

tion of an anomaly of less than 50 Ω -m resistivity to a depth of approximately 50 m. The subsurface lava tunnel network (Figure 1c) was followed to determine how the resistivity models were affected by the structure of the lava tunnel. Moreover, to provide additional elucidation, a number of features associated with the inner structure, like lava tunnel filling materials and dimensions, were used as well.

A resistivity value exceeding 3,000 Ω -m and even as high as 10,000 Ω -m was associated with the resistivity anomaly “A” denoting the lava tunnel and attained at ERT02, ERT03, ERT04, ERT05, and ERT08, while its depth was around

10 m. Furthermore, its diameter varies from 3 m at ERT08 to around 7 m at ERT03 and ERT04, suggesting a deep channel (Figure 1c and Figure 7).

Detected at ERT02 and ERT04 (Figure 7), the resistivity anomaly “B” exhibited a resistivity value exceeding 3,000 Ω -m reaching up to 10,000 Ω -m, with the subsurface tributary blocked by sediments being believed to represent a link to the primary lava tunnel (*i.e.* anomaly “A”) (Figure 8). The lava tunnel is likely to extent further southwards as suggested by the anomaly “D” detected at ERT06 (Figure 7), which was around 10 m deep and has a resistivity value of around 3000 Ω -m.

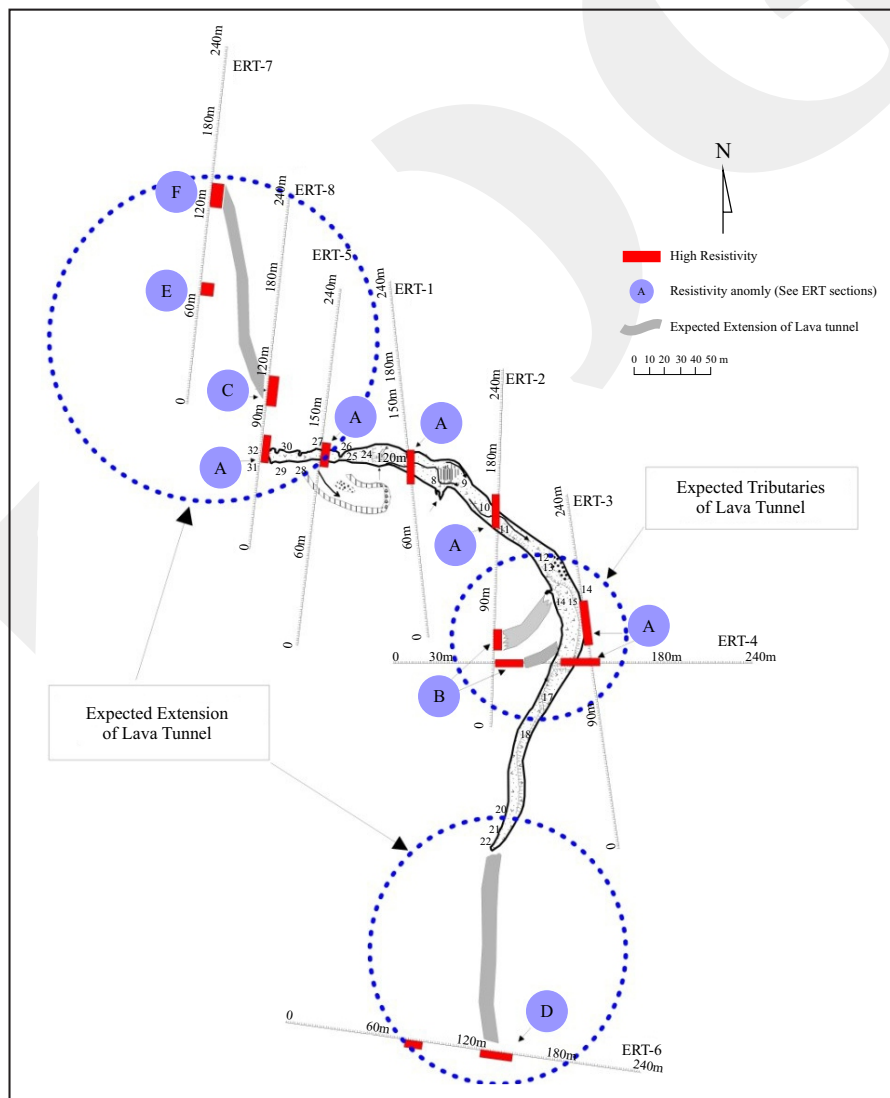


Figure 8. Inner structure of the Al-Badia tunnel (modified after Kempe *et al.*, 2006) superimposed with the sites of ERT profiles and identified resistivity anomalies. Anomaly “A” with a high resistivity indicates the tunnel, while anomalies “B”, “C”, “D”, “E” and “F” may suggest unknown tributaries of anomaly “A”.

At ERT07, anomaly “F” was detected, having a resistivity value of around 1,000 Ω -m and potentially representing a northward drift of anomaly “A”. Moreover, the formation of the resistivity anomaly “E” with a depth of 10 m was revealed by ERT07, while the formation of the anomaly “C” with a depth of 5 m was revealed by ERT08. These two anomalies could be conjectured as additional proof that the lava tunnel extends further northwards (Figure 8).

Numerous resistivity models present important conductive features (*i.e.* 3-50 Ω -m) and are associated particularly with zones underneath the resistive lava tunnel structure (*i.e.* ERT01, ERT03, ERT04, ERT07, and ERT08), as shown in Figure 7.

The derived ERT models for lava tunnel in this study can be compared to the results of other geophysical methods (*e.g.* Al - Oufi *et al.* 2008). The Very Low Frequency - Electromagnetic (VLF-EM) inverted models presented by Al-Oufi *et al.* (2008) at Umm El-Quttein area, NE Jordan, suggest very long lava tunnel extends to more than 5 km. Possible lava tunnel divergence was recorded along the survey lines. Also, the quantitative modelling of VLF data have resolved lava tunnel with resistivity of over 2,500 Ω -m, and better determined in less resistive Fahda Vesicular Basalt medium. Furthermore, the subsurface extension of lava tunnels were delineated within the first 20 m depth at all places of conducted VLF profiles and associated of multiple conductive structures of filled-sediment joints and fractures.

DISCUSSION

In northeastern Jordan, there are volcanic eruptions and basaltic lava flows dating to the Neogene-Quaternary, with associated lava tunnels and caves forming over an extensive area and recorded to a shallow depth. Consisting of the upper Fahda Vesicular Basalt Formation and the lower division of Wadi Mansif Basalt Formation, the Bishriyya Group includes most of the lava tunnels of limited depth. The characteristics of the two formations include both horizontal and

vertical joint systems, vesicles, and fresh blocky “aa” lava.

This study sought to explore interconnected underground extensions and inner structure of the Al-Badia lava tunnel, and to this end, eight ERT profiles were performed. For the purposes of target imaging, the ERT configurations and measurement of resistivity data quality employed to describe both known and unknown lava tunnels demonstrates a satisfactory efficiency. Data of good quality were obtained through the resistivity datasets based on Schlumberger and reciprocal Schlumberger with equivalence between $\pm 4\%$ of resistivity variations and 90% of reciprocal data (Figure 5). The lava tunnel was resolved in an adequately formed structure based on a maximum 10% of filtered data and application of the robust inversion routine (Figure 7).

Besides the mechanisms underpinning the development of the lava tunnel, it was observed that the setting of the lava tunnel in the researched area had a minimal ground gradient (Kempe *et al.*, 2006), which made it possible for the structure of the tunnel to be broadened (Calvari and Pinkerton, 1998; Kempe *et al.*, 2006). The variation in the dimensions of the tunnel reflects this, with the width between 10 and 20 m, the diameter between 3 and 7 m, and the depth to the ceiling of the tunnel between 5 and 13 m.

According to the geography of the Al-Badia tunnel cave, the location of the main tube-fed “aa” lava flows is at the distal part of the foremost lava flow field system, as can be seen in Figure 2. This type of lava flow spreads more widely and faster compared to other kinds of lava flows due to the low viscosity, accelerated speed, and great flow thickness given by the lava tunnel. Consequently, considerable heat is lost on the lava flow surface owing to the created lava tubes and channels (Melnik, 2017). The conclusion drawn is that the formation of the lava tunnel under investigation occurred under high discharge flux, with the earliest lava flow being induced in a northwest direction and approximately 150 km away from the researched area. Over 0.5 km of the length of the lava tunnel with 5-m average diameter was revealed by the restricted survey grid.

Besides delineating known sites along the lava tunnel, namely, anomaly "A" (Figures 7 and 8), the ERT models employed revealed the formation of a secondary lava tunnel as well, resulting from shifts in the orientation of the lava flow. It could thus be implied that there was a decrease in the original lava flow rate over effusion rate due to which a secondary drainage passages developed, namely anomalies "B", "E", and "F" (Figures 7 and 8). Kerr *et al.* (2006) investigate the behaviour of lava spreading that forms a point source using a laboratory experiment and scaling theory at a constant flow rate on a wide uniform slope. The study attributed the lava tube channelization to the ground slope, pre-existing topography, lava viscosity, lava yield strength, surface solidification, and rate of propagation.

During the formation of an air-filled tunnel, the pressure of primary lava flow maintained constant consistency and strength, ultimately resulting in self-support of the inner geometrical structure, as suggested by the fact that within the survey scale, the collapse of the lava tunnel ceiling was not represented by the ERT models. The lava tunnel exhibited well-delineated rectangular to ellipsoidal forms, high resistivity contrast, and resistivity exceeding 1,000 Ω -m within 200 Ω -m of Fahda Vesicular Basalt formation. However, in a number of areas, it has a weak and highly-jointed floor, enabling formation of a preferential path for fine sediments and surface water penetration (*i.e.* ERT01, ERT04, ERT07, and ERT08). Shawaqfah *et al.* (2014) and Al-Amoush (2010) suggested that such structures may mediate groundwater recharge. Observation of this was made at different areas with the resistivity of less than 50 Ω -m below or near the lava tunnel floor (*e.g.* ERT01 and ERT08 in Figure 7). Hence, recovery of conductive anomalies occurred solely where the resistivity of the lava tunnel was minimal (*i.e.* \sim 1000 Ω -m). So far, various lava flows with overall thickness of 600 m have been discovered in northeastern Jordan (Gibbs, 1993). The developments of near-surface and deep lava tunnels may be furthered by the Bishriyya Basaltic Group.

CONCLUSION

Focusing on the Al-Badia lava tunnel, this study proves that ERT could effectively map the underground structure of a lava tunnel. Data error quantification is based on the reciprocal error, so the recovered resistivity models have a maximal quality due to the robust signal strength up to 50 m deep supplied by the Schlumberger and its reciprocal configurations.

The resistivity models reveals that the geometry of the lava tunnel is rectangular to ellipsoidal in form, 3 - 7 m in diameter and 3 - 13 m in depth. The resistivity of the air-filled lava tunnel also varies in the range of 1,000 - 10,000 Ω -m. The lava tunnel was identified in \sim 200 Ω -m solidifying lava corresponding to the Fahada Vesicular Basalt Formation. Ellipsoidal structures with resistivity of less than 50 Ω -m are identified in numerous lava tunnel sites, especially sites where fine sediments and/or water have leached through cracks in the basaltic floor, for instance in areas where the lava tunnel or nearby sites are invaded by conductive water and fine sediments. The ERT resistivity models show that known and unknown lava tunnels are directed to the northwest and south of the researched area.

ACKNOWLEDGMENTS

The authors would like to thank Al al-Bayt University- Institute of Earth and Environmental Sciences for providing the electrical resistivity instruments. The authors would also like to thank Mr. Adnan Rizq for assisting in geo-electrical field surveys, and the reviewers are highly appreciated for their constructive comments that improve the quality of the manuscript.

REFERENCES

- Abed, A., Khoury H., and Kruhl, H., 1985. On the structure of Jabal Aritain Volcano (NE Jordan) and the petrography of some xenoliths. *Dirasat*, 12, p.109-124.

- Al-Amoush, H., 2010. Integrations of vertical electrical sounding and aeromagnetic data using GIS techniques to assess the potential of unsaturated zone and Volcanic Basaltic Caves for groundwater artificial recharge in NE-Jordan. *Jordan Journal of Civil Engineering*, 4 (4). p.389-408.
- Al-Malabeh, A., 2005. New discoveries supporting ecotourism in Jordan. In: Abstract Book, 6. Jordan, *Proceedings of 1st Economic Jordanian Forum*. Amman.
- Al-Malabeh, A., 1994. Geochemistry of two volcanic cones from the intra-continental plateau basalt of Harrat El-Jabban, NE-Jordan. *Geochemical Journal*, 28, p.517-540. DOI: 10.2343/geochemj.28.517
- Al-Malabeh, A., 1989. *The volcanic successions of Jebel Aritain volcano, NE-Jordan: A field, petrographic and geochemical study*, M.Sc. Thesis at Yarmouk University, Faculty of Sciences, Jordan, 182pp.
- Al-Malabeh, A. and Kempe, S., 2012. Hashemite University Cave, Jordan. *Proceedings of the International Symposium on Vulcanospeleology*, March 15 - 22, Jordan.
- Al-Oufi, A, Mustafa, H.A., Al-Tarazi, E., and Abu Rajab, J., 2008. Exploration of the extension of two lava tubes, faults, and dikes using very low frequency-electromagnetic technique in NE Jordan. *Acta Geophysica*, 56 (2), p.466-484. DOI: 10.2478/s11600-008-0009-y
- Al-Oufi, A., 2006. *Geophysical Exploration of Lava Tubes in Umm El-Qutein area, NE Jordan*, M.Sc. Thesis at Yarmouk University, Faculty of Sciences, Jordan.
- Al-Oufi, A., Al-Malabeh, A., and Al-Tarazi, E., 2012. Characterization of Lava Caves, Using 2D Induced Polarization Imaging, Umm Al Qutein area, NE Jordan. *Proceedings of 15th International Symposium On Vulcanospeleology*, March 15 - 22 Jordan.
- Al-Dmour, T. M., 1992. Interpreting the geology of Azraq, south area of Jordan, using landsat TM data. *Internal Report*, Geology Directorate, NRA, Jordan.
- Arsalan, F. A., 1974. *Geologie und Hydrogeologie der Azraq-Depression (Ost Jordanien)*, Unpublished Ph.D. Thesis.
- Barberi, F., Capaldi, P., Gasperini, G., Marineli, G., Santacroce, T., Scandore, R. Treuil, M., and Varet, J. 1979. Recent basaltic volcanism of Jordan and its implications on the geodynamic history of the Dead Sea shear zone. *Geodynamic Evolution of the Afro-Arabian Rift System: International Symposium*, p.667-682.
- Bender, F., 1968. *Geologie von Jordanian*, Gebrüder Bornträger, Berlin, 230pp.
- Bender, F., 1974. *Geology of Jordan. Supplementary edition in English with minor revisions*. (Gebr. Borntraeger), Berlin. 196pp.
- Binley, Ramirez, A., and Daily, W., 1995. Regularised image reconstruction of noisy electrical resistance tomography data, In: Beck, M.S., Hoyle, B.S., Morris, M.A., Waterfall, R.C., and Williams, R.A., (eds), *Process tomography: Proceedings, 4th Workshop of the European Concerted Action on Process Tomography*, p.401-410.
- Calvari, S. and Pinkerton, H., 1998. Formation of lava tubes and extensive flow field during the 1991 - 1993 eruption of Mount Etna. *Journal of Geophysical Research*, 103 (B11), p.27291-27301. DOI:10.1029/97JB03388.
- Dahlin, T. and Zhou., 2004. A numerical comparison of 2D resistivity imaging with 10 electrode arrays. *Geophysical Prospecting*, 52, p.379-398. DOI: 10.1111/j.1365-2478.2004.00423.x
- deGroot-Hedlin, C. and Constable, S., 1990. Occam's inversion to generate smooth, two dimensional models from magnetotelluric data. *Geophysics*, 55 (12), p.1613-1624.
- Doss, B., 1886. Die basaltischen laven und tuffe der Provinz Hauran und von direct Tulul in Syria. *Tschemarks, Mineralogische und Petrographische Mitteilurgen*, Neue Folge, Vienna, 7.Bd, p.461-534.
- Gibbs, B., 1993. *Hydrogeology of the Azraq basin northeast Badia, Jordan*. Unpublished M.Sc. Thesis at University College, London.
- Griffiths D.H. and Barker R.D., 1993. Two-dimensional resistivity imaging and model-

- ling in areas of complex geology. *Journal of Applied Geophysics*, 29, p.211-226. DOI: 10.1016/0926-9851(93)90005-J
- Ibrahim, K.M., 1993a. The geology framework for the Harrat Ash-Shaam Basaltic Supergroup and its volcanotectonic evolution. *Internal Report*, Natural Resources Authority, Geological Map Division, *Bulletin*, 25, p.33.
- Ibrahim, K.M., 1996a. *Geology, mineralogy, chemistry, origin and uses of the zeolites associated with quaternary tuffs of North-east Jordan*, PhD Thesis at Royal Holloway, University of London, 245pp.
- Ibrahim, K.M., 1996b. *The regional geology of Al Azraq area map sheet No. 3553 I. Scale: 1 : 50,000*, Natural Resources Authority, Geological Map division, *Bulletin*, 36, 67pp.
- Ibrahim, K., 1997. *The geology of Al Bishriyya (Al Aritayn) area map sheet No. 3553 I (with special reference to the geology of the economic zeolites deposits)*. Natural Resources Authority, Geological Map division, *Bulletin*, 39, p.54.
- Ibrahim, K. and Al-Malabeh, A., 2006. Geochemistry of El-Fada flow and the associated pressure ridges. *Journal of Asian Sciences (in press)*.
- Ibrahim, K.M., 2000. New occurrence of mantle and crustal xenoliths in the Badia Area, NE-Jordan. Submitted to *Journal of African Earth Sciences*, Elsevier.
- Ibrahim, K.M. and Hall, A., 1995. New occurrences of diagenetic faujasite in the quaternary tuff of northeast Jordan. *European Journal of Mineralogy*, 7, p.1129-1135. DOI: 10.1127/ejm/7/5/1129
- Ibrahim, K.M. and Hall, A., 1996. The authigenic zeolite of the Aritayn volcanoclastic formation, northeast Jordan, *Mineralium Deposita*, 31, p.514-522. DOI: 10.1007/BF00196131
- Ibrahim, K., Rabba, I., and Tarawneh, K., 2001. *Geological and mineral occurrences map of the northern Badia region, scale map 1:250,000, Jordan*. The Higher Council for Science and Technology, NRA, Jordan Badia Research and Development Programm, Geology Directorate Geological Mapping Division, Amman-Jordan, 136.
- Illani, S., Harlavan, Y., Tarawneh, K., Rabba, I., Weinberger, R., Ibrahim, K.M., Peltz, S., Steinitz, G., 2001. New K-Ar ages of basalt from the Harrat Ash Shaam volcanic field in Jordan: implications for the span and duration of the upper mantle upwelling beneath the western Arabian plate. *Geology*, 29, p.171-174. DOI: 10.1130/0091-7613(2001)029<0171:NKAAOB>2.0.CO;2
- Kerr, R.C., Griffiths, R.W., and Cashman, K.V. 2006. Formation of channelized lava flows on an unconfined slope. *Journal of Geophysical Research*, 111, B10206, DOI: 10.1029/2005JB004225.
- Kempe, S., Al-Malabeh, A., Frehat, M., and Henschel, H.V., 2006. State of lava cave research in Jordan. *Proceedings of the 12th International Symposium on Vulcanospeleology, Tepo, Mexico, 2 - 7 July 2006*, Mexico.
- Kempe, S., Al-Malabeh, A., and Horst-Volker Henschel, H. V., 2012. Jordanian lava caves, an overview, *Proceedings, 15th International Symposium on Vulcanospeleology*, March 15 - 22, Jordan.
- Kwon, B.D., Lee, H.S., Oh, S.H., and Lee, C.K., 1998. Application of multiple geophysical methods in investigating the lava tunnel of Manjanggal in Cheju Island. *Economic and Environmental Geology*, 31, p.535-545.
- Lartet, L., 1869. *La geologie de la Palastine. These*, University of Paris, Messon, 292pp.
- Loke, M. H., Acworth, I., and Dahlin, T., 2003. A comparison of smooth and blocky inversion methods in 2D electrical imaging surveys. *Exploration Geophysics*, 34 (3), p.182-187. DOI: 10.1071/EG03182
- Loke, M. H., 2002. RES2DINV ver. 3.54. Rapid 2-D resistivity and IP inversion using the least square method. Geotomo Software.
- Loke, M. H., 2013. Tutorial: 2-D and 3-D electrical imaging surveys. Available at www.geoelectrical.com.
- Melnik O., 2017. Flow rate estimation in a lava tube based on surface temperature measurements, *Geophysical Journal International*, 208, p.1716-1723. DOI: 10.1093/gji/ggw475
- Miyamoto H., Haruyama, J., Rokugawa, S., Oni-

- shi, K., Toshioka, T., and Jyun-ichi, K.J., 2003. Acquisition of ground penetrating radar data to detect lava tubes: preliminary results on the Komoriana cave at Fuji volcano in Japan, *Bulletin of Engineering Geology and the Environment*, 62 (4), p.281-288. DOI: 10.1007/s10064-002-0182-1
- Moffat, D.T., 1988. A volcanotectonic analysis of the Cenozoic continental basalts of northern Jordan; implications for hydrocarbon prospecting in the block B area. *ERI Jordan EJ88-1*, 73pp.
- Gómez-, O.D., S., Martín-Velázquez, T., Martín-Crespo, A., Márquez, J., Lillo, I., López, F., Carreño, F., Martín-González, R., Herrera, and De Pablo, M.A., 2007. Joint application of ground penetrating radar and electrical resistivity imaging to investigate volcanic materials and structures in Tenerife (Canary Islands, Spain). *Journal of Applied Geophysics*, 62, p.287-300. Natural Resources Authority (NRA). 2008. *Internal open files*. www.nra.gov.jo. DOI: 10.1016/j.jappgeo.2007.01.002
- Gómez-, O.D., S., Montesinos, F.G., Solla, C.M., Arnosó, J., and Vélez, E., 2014. Combination of geophysical prospecting techniques into areas of high protection value: Identification of shallow volcanic structures. *Journal of Applied Geophysics*, 109, p.15-26. DOI: 10.1016/j.jappgeo.2014.07.009
- Ramirez A., Daily W., Binley A., and LaBrecque D., 1999. Electrical Impedance Tomography of Known Targets. *Journal of Environmental and Engineering Geophysics*, 4, p.11-26. DOI: 10.4133/JEEG4.1.11
- Shawaqfah, M.I., Alqdah, I., and Nusier, O.K., 2014. Water Resources Management Using Modeling Tools in Desert Regions: The Azraq Basin, Jordan. *International Journal of Modeling and Optimization*, 5 (1), p.55-58. DOI: 10.7763/IJMO.2015.V5.436
- Tarawneh, K., Ilani, S., Rabba, I., Harlavan, Y., Peltz, S., Ibrahim, K., Weinberger, R., and Steinitz, G., 2000. Dating of the Harrat Ash Shaam Basalts Northeast Jordan (Phase 1). *National Resources Authority and the Geological Survey of Israel*.
- Van Den Boom, G. and Sawwan, O., 1966. Report on geological and petrological studies of the plateau basalts in NE Jordan. *German Geological Mission, Amman*, 42pp.
- Wilkinson, P., Jonathan, E., Chambers, Lelliott, M., Gary P., Wealthall, Richard, and Ogilvy, D., 2008. Extreme sensitivity of crosshole electrical resistivity tomography measurements to geometric errors. *Geophysical Journal International*, 173 (1), 1, p.49-62. DOI: 10.1111/j.1365-246X.2008.03725.x.
- Zhou, B. and Dahlin, T., 2003. Properties and effects of measurement errors on 2D resistivity imaging surveying. *Near Surface Geophysics*, 1 (3), p.105-117. DOI: 10.3997/1873-0604.2003001